STM JOURNALS

Journal of
Polymer & Composites

ISSN: 2321-2810 (Online)
ISSN: 2321-8525 (Print)
Volume 13, Issue 4, 2025
DOI (Journal): 10.37591/JoPC

http://engineeringjournals.stmjournals.in/index.php/JoPC/index

Research JoPC

Novel Poly (Methyl Cellulose-G-Acrylamide)/Sodium Alginate Based Zeolite 4A Filled Mixed Matrix Membranes for The Separation of Water-Isopropyl Alcohol Mixtures by Pervaporation

Saraswathi Mekala[1,*]

Abstract

The Filled blend matrix membranes of (Methyl Cellulose-g-Acryl amide)/Sodium Alginate {(MC-g-AAm)/NaAlg} prepared via solution casting method by in situ incorporation with 4A zeolite particles in 5, 10 and 15 mass % with respect to the weight of (MC-g-AAm)/NaAlg membrane. Several analytical tools such as scanning electron microscope (SEM), atomic force microscope (AFM), Fourier transform infrared spectroscopy (FTIR), X-ray powder diffraction (XRD), X-ray photoelectron spectroscopy (XPS), and thermo-gravimetric analysis (TGA) were employed for characterization of as prepared bled 4A zeolite incorporated (MC-g-AAm)/NaAlg copolymers. Glutaraldehyde was used to cross-link these membranes, which were then assessed for pervaporation (PV) dehydration of isopropanol at 30°C. Infinite separation factors and moderate fluxes were achieved with the filled matrix membranes over the studied feed composition range of 10-50 mass % water in the feed at 30^0C with the complete removal (100 mass %) of water on the permeate line with a slight compromise in flux. The PV separation performance of the (MC-g-AAm)/NaAlg was remarkably improved with high selectivity by the incorporation of 4A zeolite into membrane formulation, which enhances the hydrophilicity of the membrane due to the formation of intermolecular hydrogen bonding between zeolite and amide, carboxyl and hydroxyl functional groups of the membrane.

Keywords: Pervaporation separation; biodegradable polymers; synthesis of polymers; sodium alginate; 4a zeolite

INTRODUCTION

Mixed matrix membranes (MMM) have gained attention in recent years as an effective morphology for pervaporation. They are fabricated by incorporating filler materials like carbon molecular sieves [1,2], zeolites [1-4], or conductive polymers [5,6] into a polymer matrix. Considerable research has focused on developing membranes with zeolites as fillers due to their unique size and shape. Zeolites are hydrated aluminosilicates that exhibit molecular sieving effect and at the same time, they possess good thermal and chemical stability. Several previous studies have been devoted to molecular gas and liquid separations using zeolite-filled polymeric membranes [7-9]. Zeolites form uniform molecular sized pores and hence, separation through such materials, particularly when incorporated into polymeric matrices, the following effects like molecular sieving, selective adsorption and differences in the diffusion rates between feed

***Author for Correspondence**
Saraswathi Mekala
E-mail: saraswatidevi_m@yahoo.co.in

[1]Associate Professor, Department of Humanities &Sciences, KPRIT College of Engineering affiliated to Osmania University, Ghan Pur, Ghatkesar, Hyderabad, Telangana, India

Received Date: January 20, 2025
Accepted Date: March 18, 2025
Published Date: June 20, 2025

Citation: Saraswathi Mekala. Novel Poly (Methyl Cellulose-G-Acrylamide)/Sodium Alginate Based Zeolite 4A Filled Mixed Matrix Membranes for The Separation of Water-Isopropyl Alcohol Mixtures by Pervaporation. Journal of Polymer & Composites. 2025; 13(4): 131–152p.

liquid molecules to be separated can be achieved individually and also in combination. Type-A zeolites are highly hydrophilic, making them well-suited for organic dehydration applications [10]. The pure A type membranes prepared have the non-zeolite pores [11-12], which contain hydrophilic silanol groups and this hydrophilic property will enhance the preferential permeation of water molecules over organic components with high separation factors. Such properties are sensitive and efficient to permeate out the concentrated water because water concentrations are often higher than 98%.

Several reports have already been established high separation factors with high fluxes for organic dehydration using NaA type zeolite membranes [13-15]. However, one of the drawbacks of zeolite membranes is its high cost of preparation, since their production is economically not feasible and hence, the zeolite-filled polymeric membranes have been widely used on a laboratory scale because these are cost-effective and easier to fabricate than pure zeolite membranes. Recently significant research has been going on PV dehydration of organics have dealt with different types of filled matrix membranes containing zeolites, mesoporous materials, clays and alumino-phosphates [16-20]. Such filled matrix membranes are known to achieve high separation factors and fluxes over those of the pristine/grafted/blend membranes. In process and chemical engineering areas, isopropanol is widely used in semiconductors and liquid crystal display industries as water removing agent and forms as an azeotrope [21], and their aqueous mixtures can be separated more effectively by PV dehydration than by conventional distillation. Presently, PV is applied to dehydration of organic solvents, which works best when water content in the feed mixture is low. Thus, reversible reactions that produce water as a by-product are a good means of pervaporation for reaction enhancement. However, published reports on PV separation of water ethanol and water-acetic acid mixtures using modified polymer membranes could not offer high flux and separation factors [22-30].

In order to overcome these problems and as a part of research on membrane based separations, we present here the PV dehydration data on methyl cellulose-grafted-acrylamide (MC-gAAm) / NaAlg membrane loaded with hydrophilic microporous 4A zeolite particles and membranes were crosslinked with glutaraldehyde and tested for pervaporation (PV) dehydration of isopropanol at 30 ^{0}C. These membranes were proven to be very effective in completely dehydrating isopropanol from aqueous solution. Based on our results, the proposed method is not only an economically competitive but also environmentally benign to an enhanced pervaporation performance. The PV performances of the mixed matrix membranes obtained in this study are much better than (MC-g-AAm)/NaAlg membrane in separating water and isopropanol mixture having water at a concentration of 10-50% by mass. The flux and separation factor values obtained are discussed in terms of membrane-filler and membrane-solvent interactions. Overall, the study demonstrates the applicability of 4A zeolite filled (MC-g-AAm)/NaAlg membranes in the effective dehydration of isopropanol from their aqueous stream.

EXPERIMENTAL

Chemicals

Sodium alginate (NaAlg), methyl cellulose (MC, weight-average molecular weight-457,000), acrylamide (AAm), glutaraldehyde (GA; 25% content in water, extrapure grade), acetone, hydrochloric acid (HCl; 35% content), isopropyl alcohol (IPA), potassium persulfate (KPS or $K_2S_2O_8$) and 4A zeolite were purchased from Sigma-Aldrich, USA. All chemicals used in this study were of reagent grade and utilized without further purification. Throughout the research, double-distilled water was employed.

Membrane Preparation

Synthesis of MC-g-AAm copolymer

The grafted copolymer was prepared according to earlier procedure with some modifications [31]. In a typical procedure, 0.6 g of methyl cellulose was added in a beaker containing 100 mL of DI water. Ultrasonicate the beaker until a uniform solution is obtained, then transfer it into a 250 mL round-bottom flask (RBF). The solution temperature was slowly raised up to 60 ^{0}C under an inert nitrogen atmosphere. Then, 2.4 g of acryl amide, and 10 mL of 0.1 M potassium persulfate ($K_2S_2O_8$) were subsequently injected into the RBF and maintained the reaction temperature between 50 and 60 ^{0}C for

4h. The MC-g-AAm polymer was formed as a yellow color precipitation by the addition of 98 % methanol and filtered. The solid copolymer was dried at 40°C in an electrically controlled oven before further use.

Preparation Of Blend 4A–Zeolite Incorporated (MC-G-Aam)/Naalg Composite Copolymer Membranes

Typically, 4 g of (MC-g-AAm)/NaAlg (75:25) was dissolved in four different beakers containing 80 mL of DI water with constant stirring. Then, different amounts of 4A type zeolite filler particles at 5, 10 and 15% by weight with respect to weight of (MC-g-AAm)/NaAlg were weighed separately and dispersed in separate beakers containing 20 mL of DI water. Sonicate the 4A-type zeolite solution mixture thoroughly for 30 minutes at room temperature before adding it to the (MC-g-AAm)/NaAlg solution. The resulting reaction mixture was then continuously stirred for an additional 24 hours at room temperature. Finally, the solution was poured onto a glass plate to cast the membranes, which were dried at room temperature and then peeled off. The dried membranes immersed in a crosslinking bath containing 75% aqueous-acetone mixture along with 2.5 mL of GA and 2.5 mL of 0.1N HCl. After keeping the membranes in a crosslinking bath for about 10-12 h, they were removed, washed repeatedly with DI water and dried in an oven at 40 ^{0}C. Membrane thickness were measured by micrometer screw gauge at different positions with standard errors being < ±1.0 μm.

Characterization

The scanning electron microscopy (SEM) images were obtained using S-4700, HITACHI, Japan with attached an energy-dispersive X-ray detector at an accelerating voltage of 20 kV. The morphological roughness changes on the surface of polymers through contact mode were examined using atomic force microscopy (AFM) with a JPK NanoWizard II bioatomic force microscope, Berlin, Germany. Fourier transform infrared (FTIR) spectra of the as-prepared polymeric samples upon insertion of 4A zeolite particles were recorded using a Bruker vortex high resolution 70 FTIR spectrometer, equipped with BRUKER FT-IR Vertex 70 with a micro plate extension HTS-XT and ATR-units, from Billerica, MA, USA. X-ray diffraction (XRD) patterns of the polymers before and after treatment with 4A zeolite were analyzed using Rigaku Rint 2200 Series X-ray Automatic Diffractometer (Cu Kα radiation at a wavelength of 1.5406 Å with 40 kV, 30 mA, increment = 0.05°, scan speed = 3 deg/min) from Texas, USA. The X-ray photoelectron spectroscopy (XPS) theta probe base system with a monochromatic Al Kα line X-ray setting (200 μm, 50 W, 15 kV and parallel angle resolved XPS (PARXPS)) from Thermo Fisher Scientific Co., USA, was employed for the complete structural and elemental composition of the polymers after insertion of 4A zeolite. Thermogravimetric analysis (TGA) and Differential scanning calorimetry (DSC) were done on a TA instruments, Q-600 and Q-100 model respectively from USA. The experiment was conducted with a heating rate of 10°C/min under a nitrogen atmosphere, covering a temperature range of 20–600°C. The samples were dried by using a hot air oven from Thermo Fisher Scientific Co., USA. Two-stage vacuum pump (Toshniwal, Mumbai, India) maintained with (1.34×10^3 Pa (10 Torr)) and employed for the downstream vacuum process. The samples flux with permeate were weighed on a digital microbalance (model AE 240, Mettler, Greifensee, Switzerland; accuracy = 10^{-4} g). The refractive index (RI) and *nD* (measured using the D-line of sodium at a wavelength of 589 nm) were determined using a thermostatically controlled Abbe refractometer (Atago 3T, Japan) with an accuracy of ±0.001.

Sorption Studies

Circular disk-shaped membranes (diameter = 2.5 cm) were dried in a vacuum oven at 30°C for 48 hours before use. The membranes were then placed inside specially designed airtight test bottles containing 20 cm³ of the test solvent. These bottles were kept in an oven maintained at a constant temperature of 30°C and equilibrated by soaking in various feed mixture compositions for 48 hours. After equilibration, the swollen membranes were immediately weighed using a digital microbalance. Before weighing, any surface-adhered liquid droplets were carefully removed by gently pressing the membranes between filter paper wraps. To minimize errors due to evaporation losses, the weighing

process was completed within 15–20 seconds. Subsequently, the total swelling or equilibrium swelling (S) of the membrane was calculated using the initial dry mass (W_0) and the equilibrium mass (W_∞) of the membrane, as given by:

$$\% DS = \left(\frac{W_\infty - W_0}{W_0}\right) X\ 100 \quad (1)$$

Pervaporation Experiments

The pervaporation (PV) experiments were conducted using a custom-built apparatus, as depicted in Figure 1 [32,33]. The membrane's effective surface area in contact with the feed solution was 32.43 cm², while the feed compartment had a capacity of approximately 250 cm³. To ensure a stable operating temperature, a thermostatic water jacket was used to regulate the temperature of the feed mixture. On the downstream side of the setup, a two-stage vacuum pump was employed to maintain a vacuum pressure of 1.34×10^3 Pa (10 Torr). Prior to initiating the PV experiments, the membrane was equilibrated with the feed mixture for approximately 2 hours. The methodology followed for conducting the PV experiments aligns with the approach previously described by Chowdoji Rao and colleagues [33,34]. Once a steady state was reached, the permeate was collected at regular intervals in a trap immersed in a liquid nitrogen jar on the downstream side. The permeation flux (J) was determined by weighing the collected permeate and using the following equation:

$$J_p = \frac{Wp}{At} \quad (2)$$

Pervaporation selectivity, (α_{PV}) was calculated as,

$$\propto_{PV} = \left(\frac{P_A}{1 - P_A}\right)\left(\frac{1 - F_A}{F_A}\right) \quad (3)$$

FA represents the weight percentage of water in the feed, while PA denotes the weight percentage of water in the permeate. To ensure accuracy and reproducibility, at least three independent measurements of flux and selectivity were conducted under identical temperature and feed composition conditions, confirming the steady-state pervaporation process.

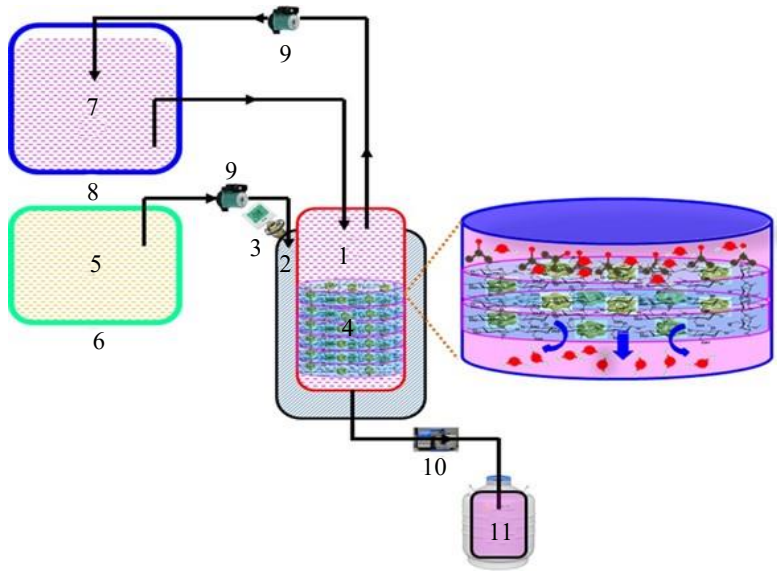

Figure 1. Schematic representation of indigenously designed apparatus for pervaporation unit: (1) feed compartment, (2) thermostatic water jacket, (3) temperature constant valve, (4) test membranes, (5) DI water, (6) Water tank, (7) feed mixture (water and IPA mixture), (8) feed mixture tank, (9) circulating pump, (10) two stage vacuum pump, and (11) liquid nitrogen tank.

Measurement of the Refractive Index (RI)

The refractive index was determined using a refractometer equipped with hollow prism casings, allowing water circulation to maintain temperature stability. The prism casing temperature was monitored using a digital display with a precision of ±0.01°C. The instrument featured two prisms, one positioned above and the other in front of the telescope. A small drop of the test liquid was introduced using a hypodermic syringe. Upon insertion, the incident ray created a distinct boundary between the illuminated and dark regions of the field, which could be observed through the telescope. This boundary shifted along the scale, enabling direct measurement of the refractive index (nD) from the instrument. The permeate composition was determined by the measurement of RI and its comparison with an established graph of RI versus mixture composition.

RESULTS AND DISCUSSION

The graft copolymerization of MC with AAm was attempted by persulfate induced radical polymerization. However, the solution viscosity decreased rapidly in a short time after being addition of 0.1 M KPS solution into the RBF at 60 ^{0} C. It could be seen that KPS is a very effective reagent in degrading the MC. The KPS would decompose into two anionic free radicals when heated as ascribed in the equation.

$$K_2S_2O_8 \rightarrow 2\ SO^{-}{}_4^{\bullet} \quad (4)$$

Eventually those free radicals were responsible for the degradation of MC to form MC-g-AAm copolymers in the presence of AAm as illustrated in the reaction Figure 2A. On the other hand, Figure 2B shows the formation of blend 4A zeolite incorporated (MC-g-AAm)/NaAlg membranes by the reaction between MC-g-AAm and NaAlg in the presence of GA and 4A zeolite. Initially, NaAlg and MC-g-AAm were connected by the GA in presence of HCl through O, O-acetal and amide bonds respectively. Finally, blend 4A zeolite incorporated (MC-g-AAm)/NaAlg membranes were formed after addition of 4A zeolites into the polymer matrices through the intermolecular hydrogen bonding between amide, carboxyl and hydroxyl functional groups of the polymers and zeolite.

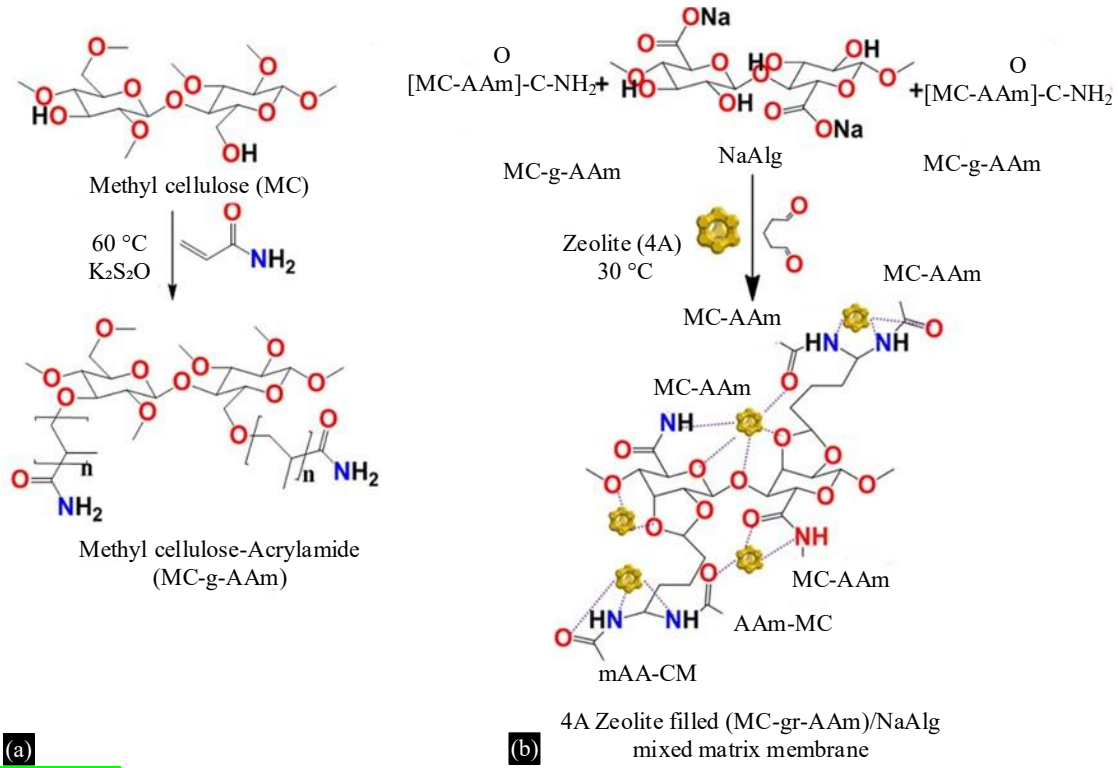

Figure 2. Illustration of reaction scheme for graft copolymerization (A), and blend 4A zeolite incorporated (MC-g-AAm)/NaAlg membranes (B).

Morphological Studies

The surface morphological and roughness of as-prepared (MC-g-AAm)/NaAlg membranes with different wt% of 4A zeolite incorporations into the polymeric matrix were examined using a scanning electron microscope (SEM) and atomic force microscope (AFM) as illustrated in Figure 3 (A) and (B) respectively. It can be seen from the SEM images that as-prepared pure (MC-gAAm)/NaAlg membrane has smooth and uniform surface matrix with defect less (Figure 3 (i)). However, significant surface roughness was increased upon incorporation of 5 (Figure 3 (iii)), 10 (Figure 3 (v)), 15 wt% of 4A zeolite (Figure 3 (vii)) into the (MC-g-AAm)/NaAlg membranes polymeric matrices. In addition, AFM was also employed to establish the surface morphology changes over the addition of different wt% of 4A zeolite into the membranes with roughness height. Figure 3 (ii) shows that pure (MC-g-AAm)/NaAlg membranes were formed uniformly with the roughness height of 8 nm. Moreover, as explained before for SEM, similar kind of increment in surface roughness with the height 10, 12 and 60 nm were observed after being addition of 5 (Figure 3 (iv)), 10 (Figure 3 (vi)), and 15 wt% of 4A zeolite (Figure 3 (viii)) into the (MC-g-AAm)/NaAlg membranes polymeric matrices respectively.

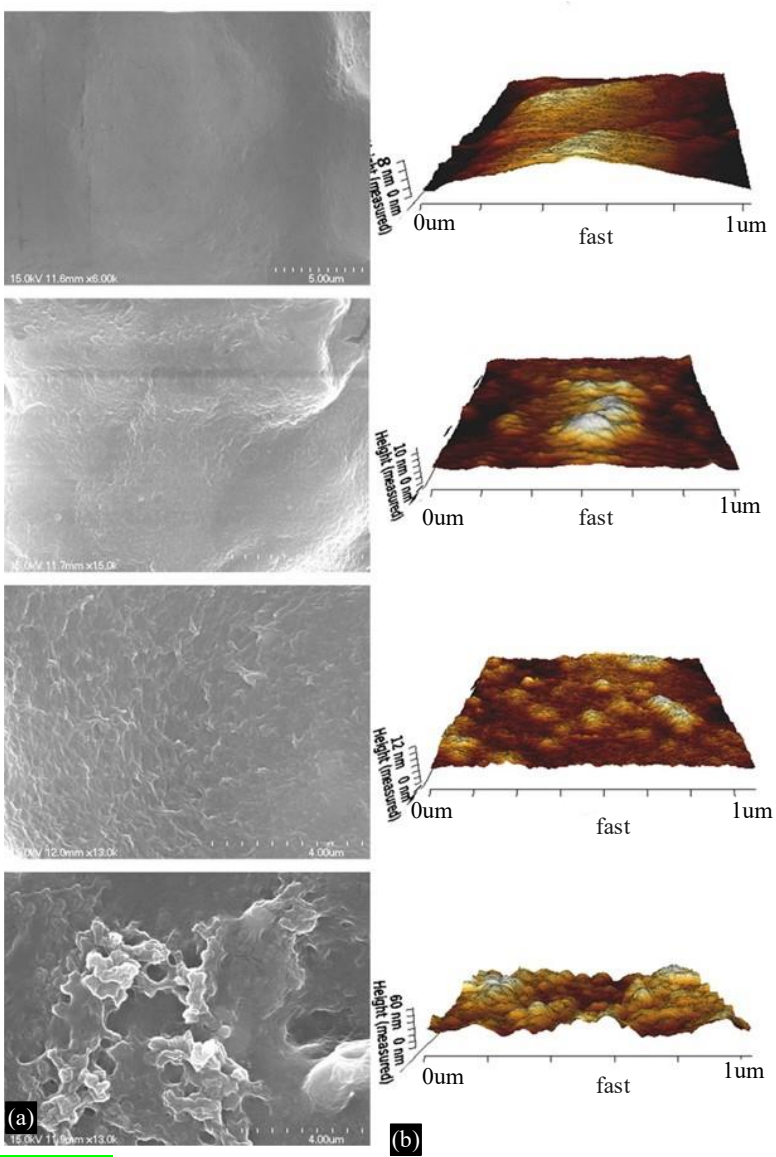

Figure 3. Surface morphology representative of (A) SEM and (B) AFM images of polymeric membranes prepared with (i, ii) pure (MC-g-AAm)/NaAlg, (iii, iv) (MC-g-AAm)/NaAl with 5 wt% 4A zeolite, (v, vi) (MC-g-AAm)/NaAlg with 10 wt% 4A zeolite and (vii, viii) (MC-g-AAm)/NaAlg with 15 wt% 4A zeolite.

However, there was a dramatic change in the surface thickness of (MC-g-AAm)/NaAlg membrane with 15 wt% of 4A zeolite due to the well incorporation of zeolite particles into the polymeric matrix. An EDX analysis was performed at different regions over the surface of polymer matrices (Figure 4). As explained earlier, the elemental peaks of Si, Al, and O intensities were increased dramatically after incorporation of different wt% of 4A zeolites into the polymeric matrices when compared with pure 4A zeolite. The in situ chemical composition of the membranes with different wt% of 4A zeolites were good agreement with the X-ray photoelectron spectroscopy (XPS).

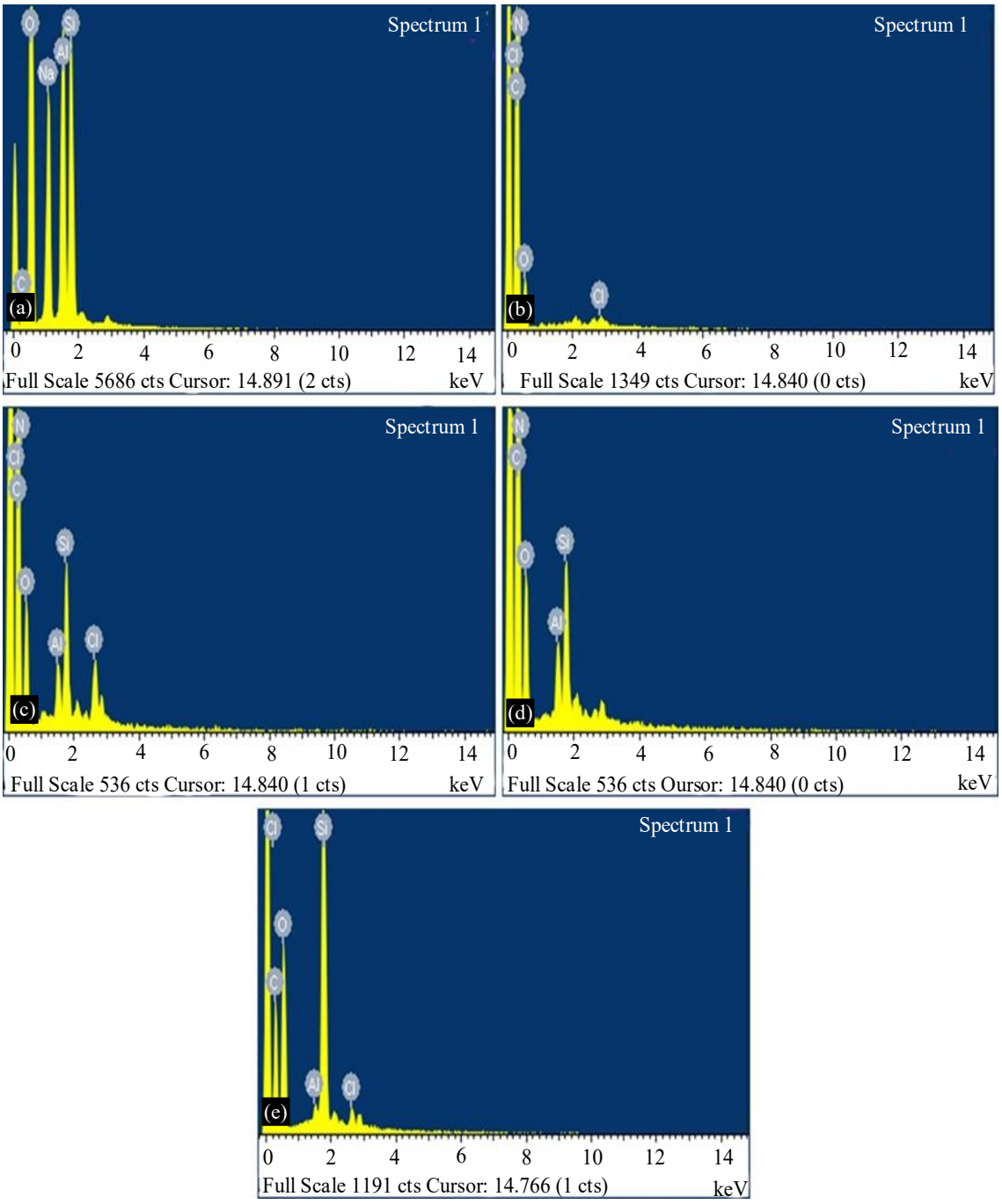

Figure 4. EDX elemental composition of (A) 4A zeolite, (B) pure (MC-g-AAm)/NaAlg, (C) (MC-g-Aam)/NaAl with 5 wt% 4A zeolite, (D) (MC-g-AAm)/NaAl with 10 wt % 4A zeolite, and (E) (MC-g-AAm)/NaAl with 15 wt% 4A zeolite.

FTIR

The FTIR spectroscopy was employed to investigate the functional group changes in the membranes before and after incorporation of 4A zeolite as shown in Figure 5. The characteristic peaks for (curve a) around 3600, and 2950 cm^{-1} are corresponding to O-H, and C-H stretching vibrations respectively. In addition, there was an intense band appeared around 1095 cm^{-1} attributed to the C-O-C of O-CH_3 groups, which is characteristic esters of methyl cellulose. The IR spectra of acrylamide (curve b) feature a broad bands at 3177 and 3345 cm^{-1} corresponding to, hydrogen bonded, primary amine, coupled doublet N-H symmetric and asymmetric stretching vibrations respectively. Meanwhile, additional bands at 1667, 1608, 1425 cm^{-1} were assigned stretching vibrations of N-H amide band I, band II, and C=C groups respectively. In the case of MC-g-AAm (curve c), the peaks of 3345, 3177, 1667, and 1608 cm^{-1} were shifted to 3426, 3060, 1715, and 1677 cm^{-1} respectively, and new peak appeared at 1453 cm^{-1} corresponding to the OCH_2. Formation of the new peak, clearly indicates the acrylamide successfully attached to the hydroxyl functional groups of methyl cellulose. On the other hand, the IR spectrum of sodium alginate (curve d) the bands representing of the C-O, COOH, C-H, and O-H groups occur at 1035, 1728, 2937, 3426 cm^{-1} respectively. Typically, 4A zeolites (curve e) processes the characteristic broad and sharp bands at 3640, and 1008 cm^{-1} for Si-O-H or Si-OH-Al and or -OH hydroxyl and Si-O-Al or Si-O-Si groups respectively.

However, significant changes have been occurred after being incorporations of different wt% of 4A zeolite (curve f, g, h and i) into the polymer matrices. Initially, the peaks of 3640, 2937, and 1008 were shifted to 3668, 2982, and 1060 cm^{-1}, respectively, and new peaks appeared at 1406 cm^{-1}, corresponding to the amide bond, which was formed when membranes were immersed in a crosslinking bath with acetone and glutaraldehyde in HCl. Secondly, the peak intensities of the curves (f, g, h and i) were dramatically decreased after addition of different wt% of 4A zeolite into the polymer matrices. Finally, in contrast to the carboxyl peak of sodium alginate was shifted to 1720 cm^{-1} after addition of 4A zeolite. Based on these IR results, it can be concluding that successfully MC-g-AAm polymer was synthesized from MC and AAm and 4A zeolite was also well incorporated into the polymer matrices uniformly due to the intermolecular hydrogen bonding between amide, carboxyl and hydroxyl functional groups of the polymers and zeolite.

XRD

The crystallinity of the polymers before and after incorporation of different content of 4A zeolite into their matrices were analyzed using X-ray diffraction (XRD) as shown in Figure 6. The XRD pattern of MC (line a), AAm (line b), and MC-g-AAm (line c) were showing more or less similar characteristics peaks around 2θ angle of 18-22° which is attributed to the amorphous nature of the carbon. However, significant peak broadening was observed in case of MC-g-AAm diffractogram, which may indicate the AAm was reacted with hydroxyl groups of MC. The X-ray diffraction of SA (line d) consisted of two crystalline peaks at 2θ = 10.1° and 18.5°, which were related to the semi crystalline nature of intermolecular hydrogen bonding between the alginate polymeric chains.

The XRD pattern of pristine 4A zeolite exhibit intense diffraction peaks at 2θ = 7.1°, 9.72°, 12.04°, 15.72°, 21.16°, 23.48°, 26.84°, 29.5°, and 33.8°, which attributed to the (100), (110), (111), (210), (300), (310), (321), (410), and (432) planes, respectively. On the other hand, obviously, most of the characteristic XRD peaks for 4A zeolite were disappeared after the incorporation of different wt% of 4A zeolite in (MC-g-AAm)/NaAlg copolymer matrix, and an amorphous crystallinity was appeared around 2θ angle of 13-35°. Noteworthy, it can be seen from the spectrum (line f, g, h, and i), intensity of the characteristics peaks were increased with the addition of different wt% of 4A zeolite in the (MC-g-AAm)/NaAlg copolymer matrix, which may be due to enhanced the interactions between zeolite and (MC-g-AAm)/NaAlg copolymer matrix.

XPS

To further, the X-ray photoelectron spectroscopy (XPS) was employed to characterize the in situ elemental composition of as-prepared different wt% content of 4A zeolite incorporated copolymers in a detailed manner (Figure 7). The full survey XPS spectrum of 4A zeolite (Figure 7, line i) and bare

(MC-g-AAm)/NaAlg (Figure 7, line ii) revealed the presence of four peaks, Aluminium (Al 2p), Silicon (Si 2p), Oxygen (O 1s), Sodium (Na 1s) and three peaks, Carbon (C 1s), Nitrogen (N 1s), and Oxygen (O 1s) respectively. The corresponding spectra for the (MC-gAAm)/NaAl with 5 wt% 4A zeolite (Figure 7, line iii), (MC-g-AAm)/NaAlg with 10 wt% 4A zeolite (Figure 7, line iv) and, (MC-g-AAm)/NaAlg with 15 wt% 4A zeolite (Figure 7, line v) blend copolymers exhibited elemental peaks of C 1s, N 1s, O 1s, Na 1s and Al 2p, Si 2p, comprising from the 4A zeolite which were present in the polymer matrices.

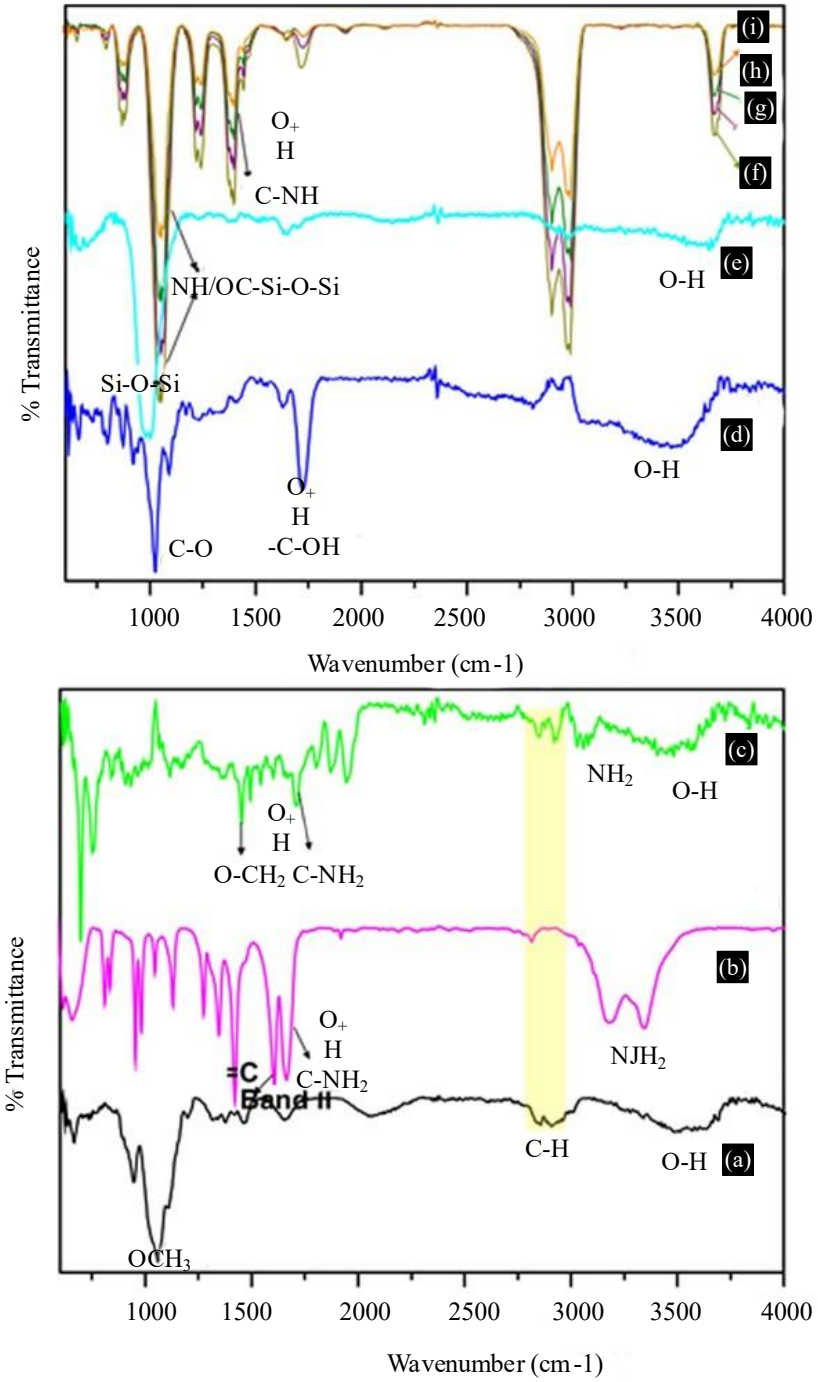

Figure 5. FTIR spectra of (a) methyl cellulose, (b) acrylamide, (c) MC-g-AAm, (d) sodium alginate, (e) 4A zeolite, (f) pure (MC-g-AAm)/NaAlg, (g) (MC-g-AAm)/NaAlg-4A (5 wt%), (h) (MC-g-AAm)/NaAlg-4A (10 wt%) and (i) (MC-g-AAm)/NaAlg-4A (15 wt%).

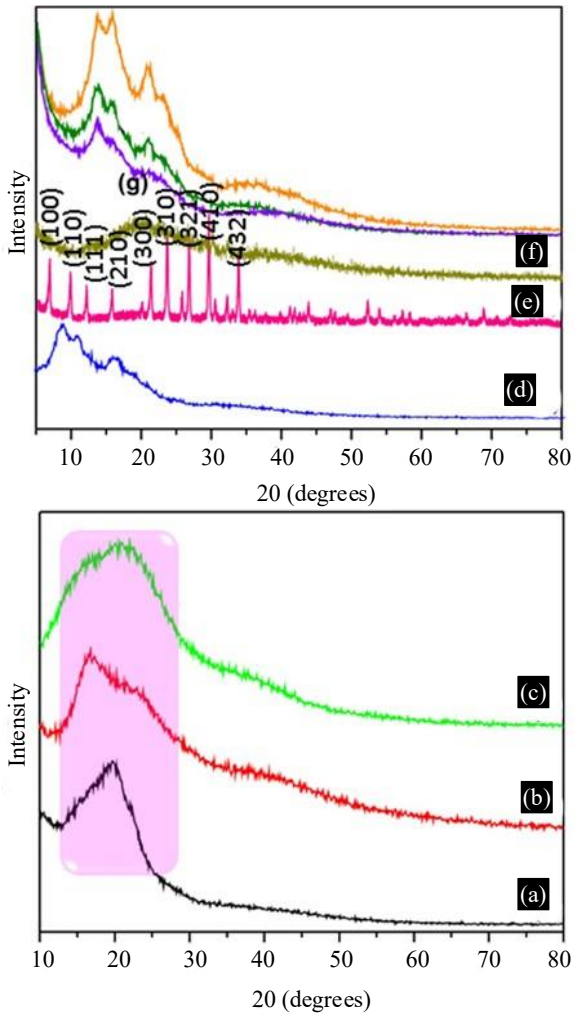

Figure 6. XRD pattern of (a) methyl cellulose, (b) acrylamide, (c) MC-g-AAm, (d) sodium alginate, (e) 4A zeolite, (f) pure (MC-g-AAm)/NaAlg, (g) (MC-g-AAm)/NaAlg-4A (5 wt%), (h) (MC-g-AAm)/NaAlg-4A (10 wt%) and (i) (MC-g-AAm)/NaAlg-4A (15 wt%).

Nevertheless, the elemental peak intensities of Al 2p (Figure 8, C-E, (i)), Si 2p (Figure 8, C-E, (ii)), N 1s (Figure 8, C-E, (iv)), and Na 1s (Figure 8, C-E, (vi)) were increased significantly after being addition of different wt % of 4A zeolite into the polymeric matrices. Moreover, these XPS elemental peak intensities were highly consistent with the obtained EDX values. In addition, the binding energies of the Al 2p (Figure 8, A (i)), Si 2p (Figure 8, A (ii)), and O 1s (Figure 8, A (v)) were slightly shifted towards high energy from 71.7, 99.8, 529.5 eV to 74, 102 and 532.5 eV respectively but in contrast, the binding energy of the Na 1s (Figure 8, C-E (vi)) was slightly shifted lower energy from 1070.5 eV to 1068.5 eV, which confirms that most of the Aluminium, Silicon, Oxygen and Sodium of zeolite were involved in the bonding with the C-OH, O=C-O, O=C-N-H polar functional groups of the polymer.

The detailed deconvolutions of high-resolution XPS data of C 1s, N 1s, and O 1s are shown in (Figure 8, B-E (iii, iv, and v)) respectively. The deconvolution of the C 1s spectrum of pure (MCg-AAm)/NaAlg polymer (Figure 8, B (iii)) shows the three peaks at 284.5, 286.7, and 288.6 eV due to the presence of C-H, C-O-C, and O-C=O functional groups respectively. The peak positions of C-H, and C-O-C were slightly shifted towards higher energy from 284.5, and 286.7 eV to 286.2 and 287.4 eV respectively and at the same time, the absence of O-C=O peak at 288.6 eV (Figure 8, C-E (iii)), upon addition of different wt% of 4A zeolite into the polymer matrices, thereby revealing that most of the O-C=O functional groups were involved in the bonding with the zeolite. In the case of nitrogen atoms for pure

(MC-g-AAm)/NaAlg (Figure 8, B (iv)), two peaks found at 398.2, and 399.4 eV were assigned to the N-H and NHC=O respectively. When compared to the bare (MC-g-AAm)/NaAlg, there was also a significant peak shifting from 398.2, and 399.4 eV to 399.2 and 400.8 eV and remarkable peak intensity decrements were observed after being addition of different content of 4A zeolite (Figure 8, C-E (iv)), indicating the Al, Si, O of zeolite may also involve bonding with the N-H and NHC=O functional groups of polymer. Finally, the high-resolution O 1s spectrum (Figure 8, B (v)) revealed the presence of two peaks corresponding to C=O and C-O-C/C-OH at 531.5 and 533.8 eV. As stated earlier, similar kind of higher energy peak shifting was also observed (Figure 8, C-E (v)), which clearly indicating the C=O and C-O-C/C-OH functional groups also involved in the bonding with zeolite. These results revealed that Al, Si, Na, O elements of zeolite were involved in bonding with the polar functional groups of C-O-C, OC=O, N-H, NHC=O, C=O and C-O-C/C-OH of the polymer matrices. Based on the comparison of deconvolution XPS study clearly showed that the polymers were formed with uniform distribution of 4A zeolite into their polymeric matrices, which was good agreement with FTIR and XRD studies. The corresponding summary of XPS elemental peak positions for as prepared polymers with and without addition of different content of 4A zeolite at a glance were shown in Table 1.

TGA

The TGA analysis of as prepared membranes before and after incorporation of 4A zeolite are presented in (Figure 9, line a-i) and corresponding weight loss thermal stability evolution is shown in (Table 2). It can be seen from the TGA analysis, the neat polymer and polymers with different wt% content of 4A zeolite gradually undergo multistage decomposition on heating in the temperature ranging from 20-600 ^{0}C. Moreover, the polymers do not explode on heating and are exhibiting an excellent thermal stability. The thermogram of the MC (Figure 9, line a), the first stage decomposition was observed in the temperature range between 30-170 ^{0}C attributed to the possible cause for the liberation of moisture and high water-retention capacity of MC.

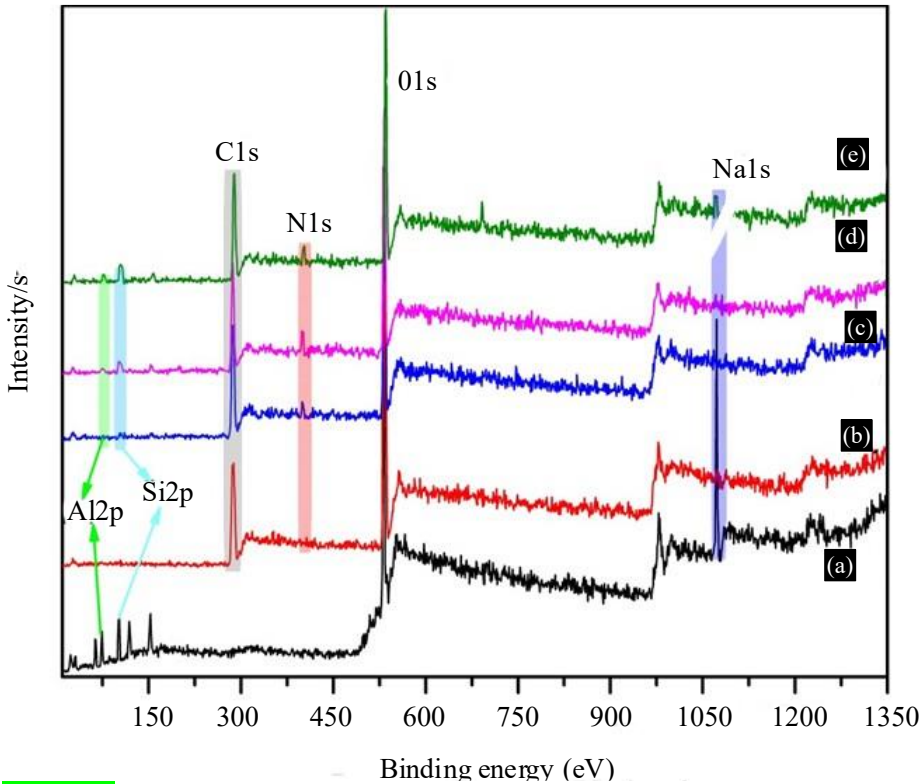

Figure 7. Typical XPS wide scan spectrum of (a) 4A zeolite, (b) pure (MC-g-AAm)/NaAlg, (c) (MCg-AAm)/NaAl with 5 wt% 4A zeolite, (d) (MC-g-AAm)/NaAlg with 10 wt% 4A zeolite and, and (e) (MC-g-AAm)/NaAlg with 15 wt% 4A zeolite.

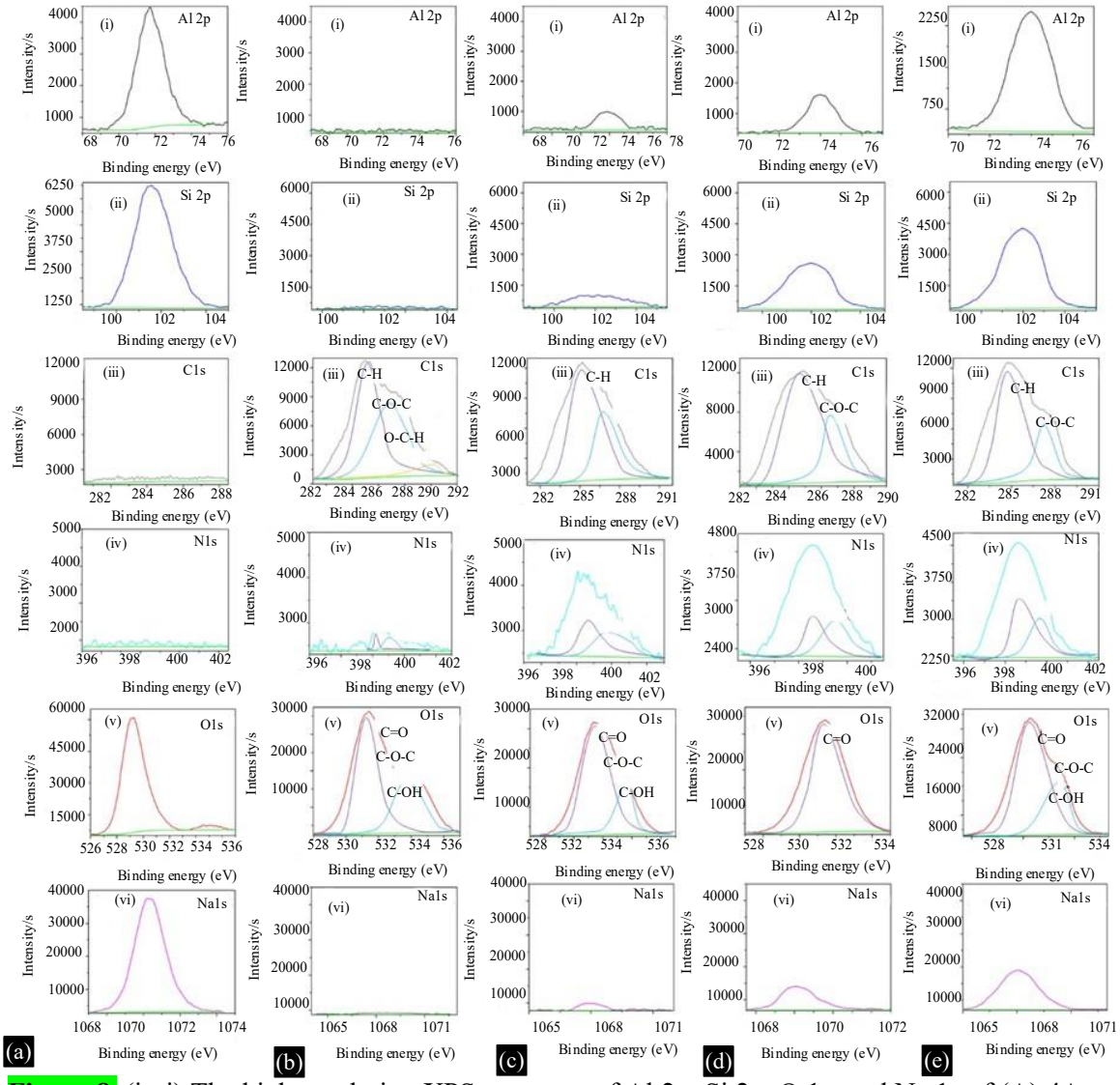

Figure 8. (i-vi) The high-resolution XPS spectrum of Al 2p, Si 2p, O 1s, and Na 1s of (A) 4A zeolite, C 1s, N 1s, and O 1s of (B) pure (MC-g-AAm)/NaAlg, and Al 2p, Si 2p, C 1s, N 1s, O 1s, and Na 1s of (C) (MC-g-AAm)/NaAl with 5 wt% 4A zeolite, (D) (MC-g-AAm)/NaAl with 10 wt% 4A zeolite, and (E) (MC-g-AAm)/NaAl with 15 wt% 4A zeolite.

The second stage of decomposition was occurred due to complete loss of MC carbohydrate back bone and carbon composition at the temperature range between 170-600 ^{0}C. In case of AAm (Figure 9, line b), the initial set of weight loss was observed at three temperature ranges 20-90 ^{0}C (0.77 %), 90 -161 ^{0}C (26.87 %), and 161-229 ^{0}C (13.18 %) due to the decomposition of water moisture, CO_2, and CO, and the next second step weight loss was occurred in three steps between 229-279 ^{o}C (5.16 %), 279-367 ^{0}C (16.70 %), and 367-600 ^{0}C (28.48 %) for AAm possibly due to loss of NH_3, C=C, and organic carbon skeleton. Interestingly, the initial weight loss has been increased up to ~220 ^{0}C for MC-g-AAm (Figure 9, line c), which clearly indicate the AAm was well reacted with the -OH functional groups of polymer and three stage decomposition was observed due to the loss of water moisture, CO_2, NH_3, and carbon skeleton at 20-216 ^{0}C, and 216-336 ^{0}C and 336-600 ^{0}C respectively. In the curve of 4A zeolite (Figure 9, line d) shows two weight loss steps at 20-264 ^{0}C and 264-600 ^{0}C. Based on weight variation, the initial weight reduction is attributed to the desorption of water, while the subsequent loss is associated with the dehydroxylation of silanol groups and the combustion of residual carbonaceous material. Weight loss was observed in four stages due to dehydration, decarboxylation, decomposition of backbone, and finally sodium bicarbonate formation to produce residues of sodium bicarbonate and

carbonized material at 20-138 ^{0}C (8.48 %), 138-225 ^{0}C (17.70 %), 225277 ^{0}C (24.61 %), and 277-600 ^{0}C (22.53 %), respectively for NaAlg (Figure 9, line e). It can be evident from the TGA thermogram that there was a little less weight loss was exhibited in the thermal decomposition up on addition of different wt% of 4A zeolite into the polymer matrices when compared with pure (MC-g-AAm)/NaAlg (Figure 9, line f). However, as expected earlier, three stage weight loss was observed for (MC-g-AAm)/NaAl with 5% 4A zeolite (Figure 9, line g), (MC-g-AAm)/NaAlg with 10% 4A zeolite (Fig. S4, line h), and (MC-g-AAm)/NaAlg with 15% 4A zeolite (Figure 9, line i) because of dehydration of water moisture, decomposition of organic moiety and dehydroxylation of silanol groups at ~20-145 ^{0}C, ~150-300 ^{0}C, and ~310-600 ^{0}C respectively. Based on TGA analysis, the thermal stability of polymers up on insertion of 4A zeolite into their matrices were significantly increases when compared to the neat grafted polymer.

Swelling Studies

Effects of feed composition and zeolite loading on membrane swelling

The study examines the effect of feed composition and zeolite loading on membrane swelling. The percentage degree of swelling data, obtained from experiments conducted at 30°C (Figure 10). These experiments were performed on (MC-g-AAm)/NaAlg membranes and 4A zeolite-filled (MC-g-AAm)/NaAlg membranes, with swelling measured as a function of the mass percentage of water in water/isopropanol mixtures. Swelling kinetics are influenced by the mutual diffusion of solvent molecules and the relaxation processes of polymer chains. In the present study, swelling increases with increasing loadings of Zeolite particles. For instance, swelling is higher for 15 mass% 4A zeolite filled (MC-g-AAm)/NaAlg membrane than those observed for 10 and 5 mass% zeolite filled (MC-g-AAm)/NaAlg and (MC-g-AAm)/NaAlg membranes; for all the hybrid mixed matrix composite membranes, swelling is higher than the unfilled (MC-g-AAm)/NaAlg membrane. Higher sorption would result in higher specific interactions, but the extent of interaction between liquid molecules with the membrane materials also depends upon the nature of the organic components of the mixed feed media. At increasing filler content, sorption also increases. These data further indicate that water molecules are sorbed preferentially and then diffused more easily through the hybrid mixed matrix composite membranes than with the unfilled (MC-g-AAm)/NaAlg membrane due to the 4A zeolite, being highly hydrophilic in nature. Thus these zeolites might be involved in specific interactions with the hydrophilic (MC-g-AAm)/NaAlg membrane, which have the higher propensity to water molecules than the organic component (i.e. isopropanol). Thus complete dehydration was achieved, since almost all of water molecules are extracted on the permeate side of the membrane.

Table 1. The elemental composition of as prepared polymers with and without addition of different content of 4A zeolite into their matrix at a glance.

S no	Type of polymer	Al 2p (eV)	Si 2p (eV)	C 1s (eV)			N 1s (eV)		O 1s (eV)		Na 1s (eV)
				C-H	***C-O-C***	***O-C=O***	***N-H***	***HNC=O***	***C=O***	***C-O-C/C-OH***	
1	4A zeolite	71.7	99.8	-	-	-	-	-	529.8		1070.5
2	pure (MC-g-AAm)/NaAlg	-	-	284.5	286.7	288.6	398.2	399.4	531.5	533.8	-
3	(MC-g-AAm)/NaAl with 5 wt% 4A zeolite	74	102	286.2	287.4	-	399.2	400.8	531.5	533.8	1068.5
4	(MC-g-AAm)/NaAlg with 10 wt% 4A zeolite	74	102	286.2	287.4	-	399.2	400.8	531.5	-	1068.5
5	(MC-g-AAm)/NaAlg with 15 wt% 4A zeolite	74	102	286.2	287.4	-	399.2	400.8	531.5	533.8	1068.5

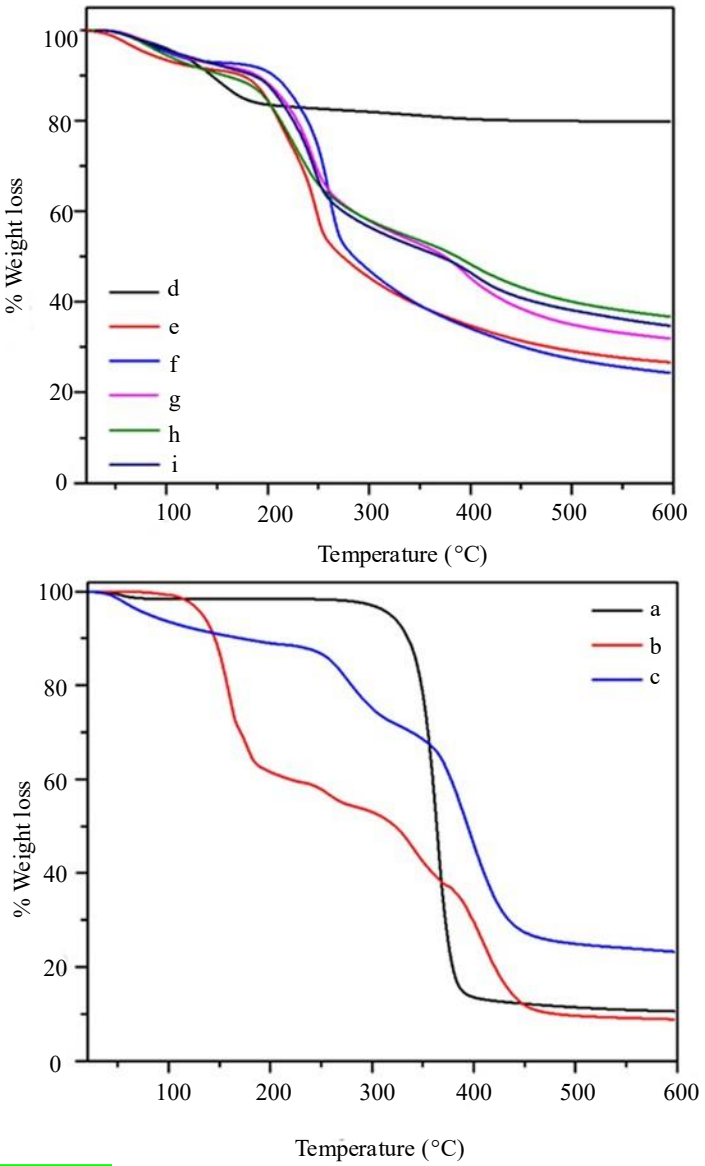

Figure 9. TGA plot of (a) methyl cellulose, (b) acrylamide, (c) MC-g-AAm, (d) sodium alginate, (e) 4A zeolite, (f) pure (MC-g-AAm)/NaAlg, (g) (MC-g-AAm)/NaAlg-4A (5 wt%), (h) (MC-g AAm)/NaAlg-4A (10 wt%) and (i) (MC-g-AAm)/NaAlg-4A (15 wt%).

Pervaporation Studies

Effect of zeolite 4A on membrane performance

The pervaporation results of the mixed matrix membrane (MMM) for the water-isopropanol feed mixture at 30°C are summarized in Table 3. The influence of zeolite loading at 5, 10, and 15 mass% in the (MC-g-AAm)/NaAlg membrane matrix was examined, as the incorporation of zeolite resulted in variations in flux and selectivity. The enhanced membrane performance of (MC-g-AAm)/NaAlg can be attributed to interactions between the filler and polymer, as well as between the membrane and solvent. The effect of zeolite content in the (MC-g-AAm)/NaAlg matrix was analyzed for feed compositions ranging from 0% to 100% water. With increasing 4A zeolite loading, both selectivity and flux exhibited an upward trend. The proposed working mechanism for water pervaporation from isopropanol is illustrated in Figure 11. This behavior can be explained by the highly hydrophilic nature of 4A zeolite, which facilitates significant water absorption through its molecular-sized pores, thereby forming preferential pathways for water transport across the membrane. Additionally, the steric hindrance and larger molecular size of isopropanol, compared to water, limit its passage through the

membrane. Hydrophilic-hydrophilic interactions further contribute to the rejection of the organic component, as isopropanol is relatively hydrophobic compared to water. Consequently, an increase in zeolite content results in higher water flux, as reflected in Table 3. The strong interaction between water molecules and the hydrophilic 4A zeolite enhances water transport across the membrane at higher zeolite loadings.Key properties of zeolite 4A, such as molecular sieving and preferential adsorption, play a crucial role in membrane separation when it is well integrated into the (MC-g-AAm)/NaAlg matrix. Moreover, interfacial interactions between zeolite and the polymer influence the overall separation efficiency. Zeolite 4A selectively differentiates components in aqueous-organic mixtures either by excluding larger competing molecules or by preferential adsorption. Thus, incorporating zeolite 4A into (MC-g-AAm)/NaAlg is expected to significantly enhance separation performance. Furthermore, from both sorption and diffusion perspectives, membranes exhibit superior selectivity for water over organic compounds. Sorption is primarily driven by hydrophilic-hydrophilic interactions, while diffusion is influenced by membrane morphology and polymer chain mobility. The presence of 4A zeolite particles in the (MC-g-AAm)/NaAlg matrix contributes to improved selectivity and flux, reinforcing the role of zeolite as a performance-enhancing additive in mixed matrix membranes.

Table 2. Thermogravimetric data for neat grafted MC-g-AAm and different wt% 4A zeolite inserted copolymers.

Compound	Temperature range (°C)	Observed weight loss (%)	Final residue (%)
Methyl cellulose (MC)	30-170	1.578	87.902
	170-600	10.52	
Acrylamide (AAm)	20-90	0.77	8.82
	90-161	26.87 13.18	
	161-229	5.16	
	229-279	16.70	
	279-367	28.48	
	367-600		
MC-g-AAm	20-216	11.47 18.71	23.20
	216-336	46.63	
	336-600		
4A Zeolite	20-264	17.66	79.86
	264-600	2.48	
Sodium alginate	20-138	8.48	26.66
	138-225	17.70 24.61	
	225-277	22.53	
	277-600		
(MC-g-AAm)/NaAlg membrane	20-144	7.15	24.17
	144-285	44.36	
	285-600	24.31	
(MC-g-AAm)/NaAl with 5% 4A zeolite	20-142	7.57	31.76
	142-273	31.70	
	273-600	28.94	
(MC-g-AAm)/NaAlg with 10% 4A zeolite	20-143	9.61	36.56
	143-315	34.53	
	315-600	19.30	
(MC-g-AAm)/NaAlg with 15% 4A zeolite	20-149	8.09	35.51
	149-273	32.83	
	273-600	24.56	

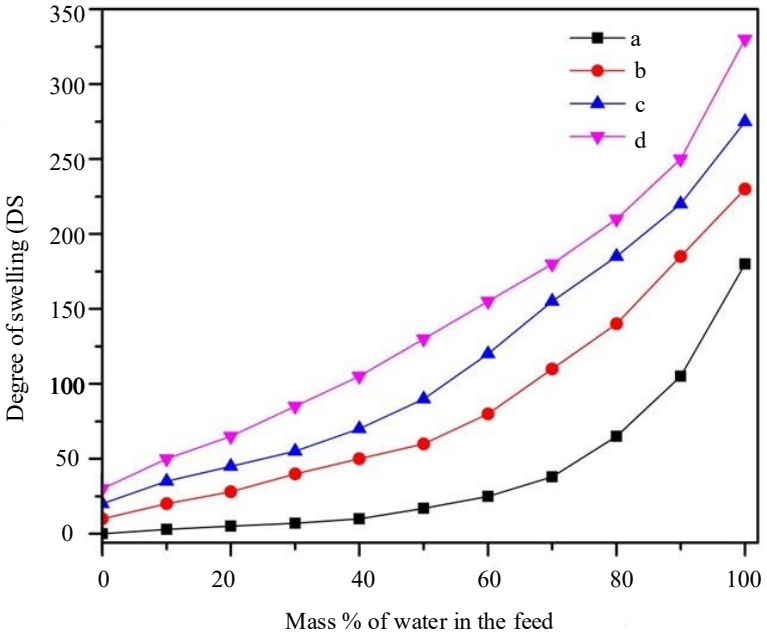

Figure 10. Degree of swelling vs mass % of water in the feed for (a) (MC-g-AAm)/NaAlg, (b) (MCg-AAm)/NaAlg-4A (5 wt%), (c) (MC-gr-AAm)/NaAlg-4A (10 wt%) and (d) (MC-grAAm)/NaAlg-4A (15 wt%) membranes at 30 ^{0}C.

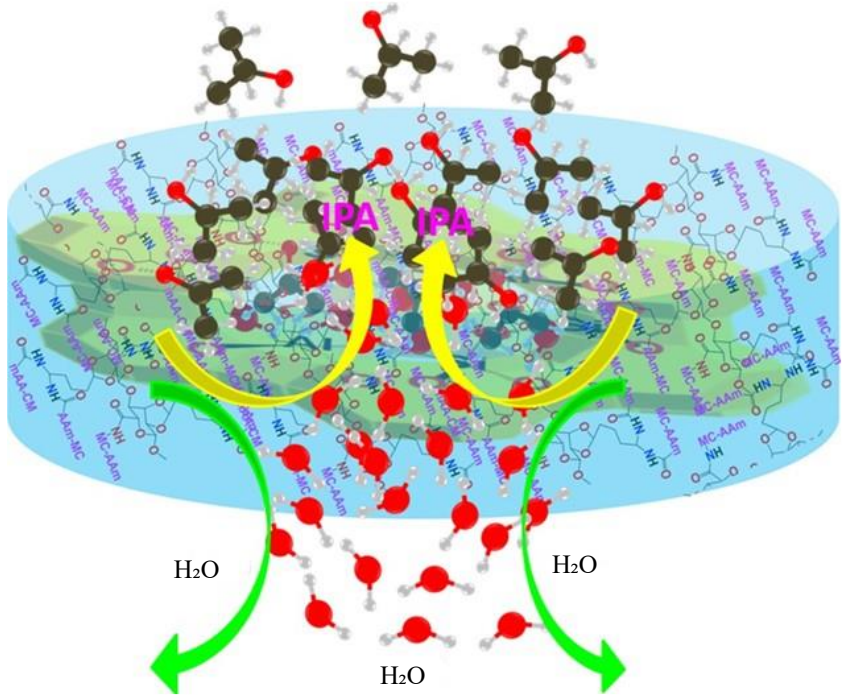

Figure 11. Illustration of plausible working mechanism for pervaporation of water from isopropyl alcohol.

Effect of Feed Composition

From the Table. 3, it is noticed that the flux values of the (MC-g-AAm)/NaAlg as well as the filled (MC-g-AAm)/NaAlg matrix membranes have increased with increasing feed water concentrations for the feed mixtures shown in Figure 12. At all the feed mixture compositions, the flux values increased with increasing content of the zeolite loadings. In case of water + isopropanol feed mixtures with water

content ranging from 10 to 50 mass%, flux of the (MC-g-AAm)/NaAlg membrane increased from 0.118 to 0.221 kg/m^{2}h. Whereas for the filled (MC-g-AAm)/NaAlg composite membranes (5, 10 and 15 mass% 4A zeolite), flux values are higher than observed for (MC-g-AAm)/NaAlg membrane and these values increased from 0.174 to 0.311 kg/m^{2}h, 0.231 to 0.395 kg/m^{2}h and 0.248 to 0.456 kg/m^{2}h respectively. The flux values are increased with increase in zeolite content and also they are higher than the unfilled membranes. Such an increase in flux for feed mixtures of this study is in accordance with the data reported on other hydrophilic membranes. This effect is the result of higher level specific interactions between water and isopropanol molecules. The lowest flux value observed for the 5 mass% 4A zeolite-loaded NaAlg membrane can be attributed to reduced surface diffusion and limited activated transport of water through the pores of the mixed matrix membranes (MMMs). However, at 15 mass% 4A zeolite loading, the increased hydrophilicity of the MMM enhances the adsorption capacity of zeolite particles, resulting in higher permeation flux.

Table 3. Pervaporation Results of 4A Zeolite filled (MC-gr-AAm)/NaAlg mixed matrix membranes in water-isopropanol mixtures.

S no.	Mass% of water in the feed	Water Flux(kg/m^2.h)	Selectivity	Mass % of water in the permeate
(MC – g - AAm)/ NaAlg membrane				
1.	10	0.118	44991	99.98
2.	20	0.128	19996	99.98
3.	30	0.157	5831	99.96
4.	40	0.190	2498	99.94
5.	50	0.221	1427	99.93
4A (5 mass%) filled (MC – g -AAm)/NaAlg membrane				
1.	10	0.174	∞	100.00
2.	20	0.216	19996	99.98
3.	30	0.262	11664	99.98
4.	40	0.278	2998	99.95
5.	50	0.311	1999	99.85
4A (10 mass%) filled (MC – g -AAm)/NaAlg membrane				
1.	10	0.231	∞	100.00
2.	20	0.276	∞	100.00
3.	30	0.342	∞	100.00
4.	40	0.349	4998	99.97
5.	50	0.395	1999	99.95
4A (15 mass%) filled (MC – g -AAm)/NaAlg membrane				
1.	10	0.248	∞	100.00
2.	20	0.371	∞	100.00
3.	30	0.411	∞	100.00
4.	40	0.433	∞	100.00
5.	50	0.456	∞	100.00

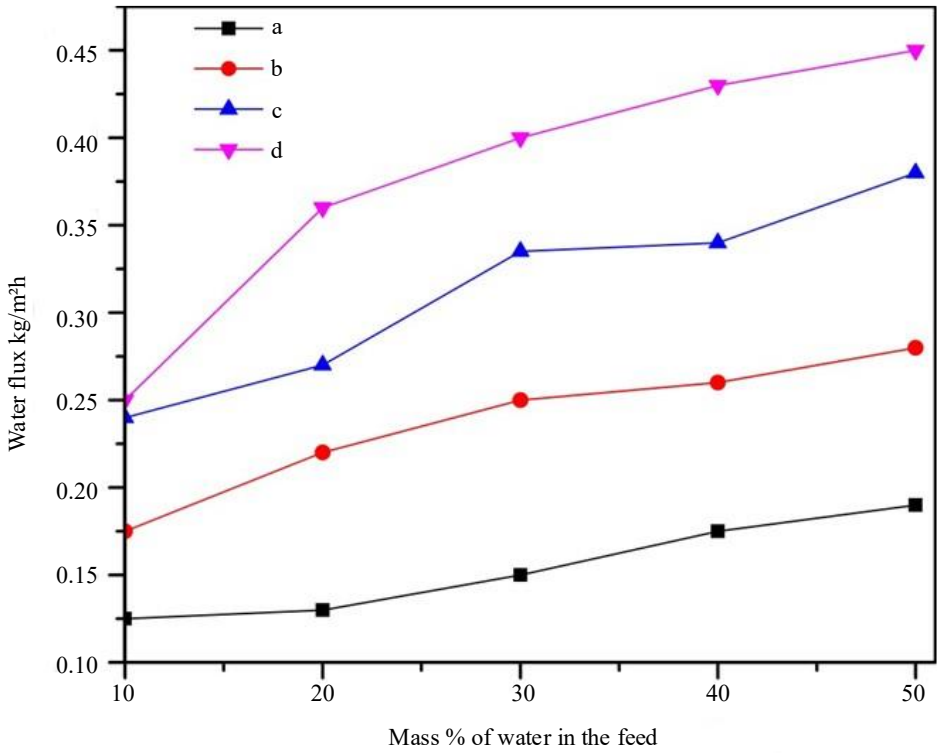

Figure 12. The Water flux vs mass % of water in the feed for (a) (MC-g-AAm)/NaAlg, (b) (MC-gAAm)/NaAl with 5 wt% 4A zeolite, (c) (MC-g-AAm)/NaAl with 10 wt% 4A zeolite, and (d) (MC-g-AAm)/NaAl with 15 wt% 4A zeolite membranes at 30 ^{0}C.

The selectivity for water-isopropanol feed increased steadily with increasing loading zeolite particles. This justifies a mark increased in selectivity to infinite with a recovery of 100 mass% of water on the permeate side for composite membranes. Composite membrane of this study is thus highly water selective, but small difference in zeolite compositions have led to high selectivity values. Figure 13 displayed the mass% of water in the permeate vs mass% water in feed. The decrease in selectivity in all the membranes with increasing the water content of the feed depends upon the amount of 4A zeolite filled (MC-g-AAm)/NaAlg. For instance, selectivity of (MC-g-AAm)/NaAlg 5 and 10 mass% of 4A zeolite filled (MC-g-AAm)/NaAlg membranes are decreased from 44991 to 1427, ∞ to 1999 and ∞ to 1999 respectively with increasing feed water composition from 1050 mass% water concentrations. Whereas for selectivity of 15 mass% 4A zeolite filled (MC-g- AAm)/NaAlg membrane have shown ∞ values to entire feed water composition ranging from 1050 mass% water concentrations, indicating the effectiveness of the membranes in dehydrating isopropanol. The composite membrane performance has increased dramatically for the dehydration of isopropanol with infinite selectivity to water. In the present study, separation depends upon the interaction between polymer matrix in addition to filler particles (4A) that have the dual pore nature and having hydrophilic functions that play independently with in the membrane matrix. Moreover, these data depend upon % loading of 4A Zeolite into (MC-gAAm)/NaAlg matrix as well as the hydrophilic nature of 4A, which further interacts with the hydrophilic (MC-g-AAm)/NaAlg matrix thus increasing its affinity to water molecules over the organic components, since water is more polar than organic components.

Comparison Studies

From a comparison of present PV data with published results shown in Table 4, there is a good improvement in selectivity of water for both mixtures for all the MMMs compared with similar type of data published in the literature. In general, one could see a good improvement in both flux and selectivity data and the differences are attributed to different experimental conditions employed by different authors, which is hard to maintain.

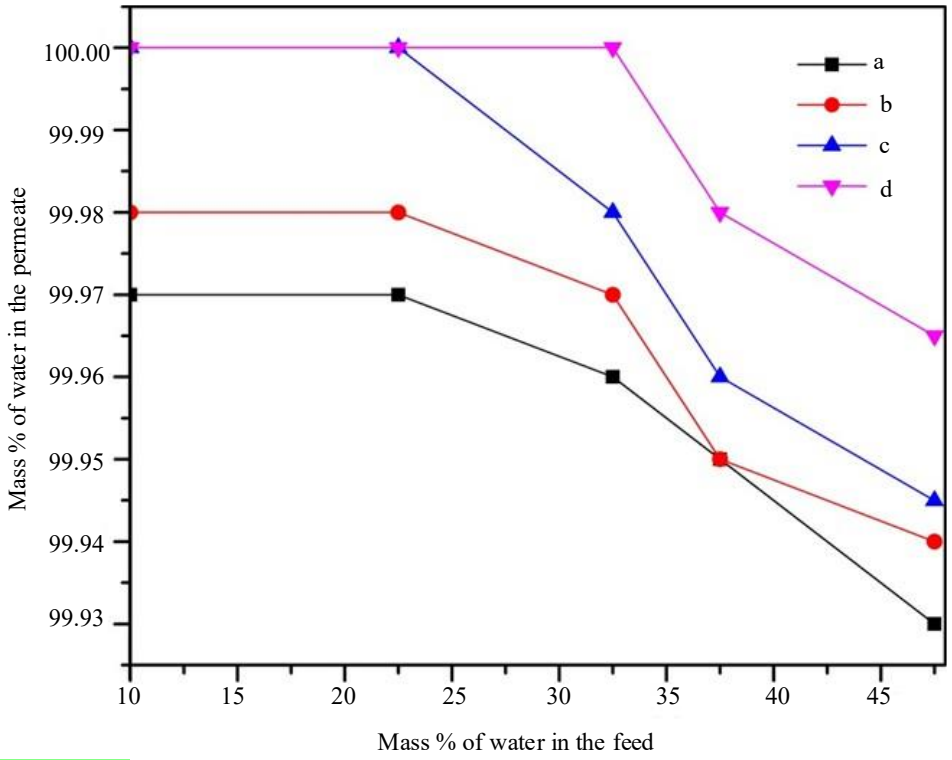

Figure 13. The mass % of water in the permeate vs mass % of water in the feed for (a) (MC-gAAm)/NaAlg, (b) (MC-g-AAm)/NaAlg-4A (5Mass %), (c) (MC-g-AAm)/NaAlg-4A (10Mass %) and (d) (MC-g-AAm)/NaAlg-4A (15Mass %) membranes at 30 ^{0}C.

Table 4. Comparison of PV performance of the present crosslinked blend membranes with literature data for water-isopropanol mixtures at 30 °C.

S no	Membrane	Mass % of water in feed	Flux (kg/m^2.h)	Selectivity	Ref.
1	NaAlg/(guargum-g-AAm) (75:25)	10	0.062	711	[35]
	NaAlg/(guargum-g-AAm) (50:50)	10	0.123	891	
	5 mass% NaY zeolite filled- NaAlg	10	0.1419	191	
2	15 mass% NaY zeolite filled- NaAlg	10	0.1607	210.51	[36]
	30 mass% NaY zeolite filled- NaAlg	10	0.2325	272.25	
3	MCM-41 (20%)-filled NaAlg	10	0.550	∞	[37]
4	PVA/BMIMCl-0.75	10	0.0224	7389	[38]
	PVA/BMIMCl-0.75	40	0.0358	1092	
5	CS grafted with PANI	10	0.0119	2092	[39]
6	TFC TbHF	15	2.65	261	[40]
7	SPVA/SPTA-15	10	0.0351	3452	[41]
8	PVA/PEC	10	1.35	1002	
9	NaAlg/(MC-g-AAm)	10	0.1185	∞	Present work
	5 mass% 4A zeolite filled-NaAlg/(MC-g-AAm)	10	0.1739	∞	
	10 mass% 4A zeolite filled-NaAlg/(MC-g-AAm)	10	0.2314	∞	
	15 mass% 4A zeolite filled-NaAlg/(CMC-g-AAm)	10	0.2484	∞	

CONCLUSION

This study highlights the impact of incorporating mesoporous materials into hydrophilic polymer matrices to analyze the permeation behavior of binary aqueous-organic mixtures of industrial significance, with a particular focus on the dehydration of organic components. The fabricated composite membranes were thoroughly characterized using SEM, AFM, FTIR, XRD, XPS, and TGA. To develop pervaporation (PV) composite membranes, well-defined molecular sieves were embedded into the (MC-g-AAm)/NaAlg matrix. The resulting membranes demonstrated high resistance to organic components while exhibiting superior permeability to water, making them highly effective in dehydrating isopropanol-water mixtures. The pervaporation performance of composite membranes containing 4A-type fillers was influenced by the interaction of the dual-pore system of the fillers, the hydrophilic nature of the (MC-g-AAm)/NaAlg matrix, and the adsorption-diffusion-desorption mechanism. The membranes exhibited a strong affinity for hydrophilic mesoporous fillers, leading to preferential water adsorption. This, in turn, restricted the transport of organic components through the hydrophilic micropores of the filler due to their specific interactions with the membrane matrix. These conditions favored the selective sorption of water molecules over organic compounds, achieving near-complete water removal on the permeate side. Given their effectiveness, the developed membranes hold potential for commercial applications, particularly in the separation of water from isopropanol in industrial processes and the extraction of water from organic pollutant-containing mixtures.

Acknowledgement

The authors are indebted to all the researchers whom we cited in this article for their significant and valuable research. No funding was received to perform this work.

Competing Interest

The authors declare no competing financial interest.

REFERENCES

1. Gao C, Zhang M, Pan F, Wang L, Liao J, Nie T, Zhao J, Cao K, Zhan L, Jiang Z. Pervaporation dehydration of an acetone/water mixture by hybrid membranes incorporated with sulfonated carbon molecular sieves. RSC Advances. 2016;6(60):55272-81.
2. S. Fazlifard, T. Mohammadi, O. Bakhtiari, Chitosan/ZIF-8 Mixed-Matrix Membranes for Pervaporation Dehydration of Isopropanol. Chem. Eng. Technol. 40 (2017) 648-655.
3. S. Li, F. Qin, P. Qin, M. N. Karim, T. Tan, Preparation of PDMS membrane using water as solvent for pervaporation separation of butanol–water mixture. Green Chem. 15 (2013) 2180-2190.
4. B. Wang, P. K. Dutta, Influence of Cross-Linking, Temperature, and Humidity on CO_2/N_2 Separation Performance of PDMS Coated Zeolite Membranes Grown within a Porous Poly(ether sulfone) Polymer. Ind. Eng. Chem. Res. 56 (2017) 6065-6077.
5. J. Wang, Z. Liu, An efficient synthetic strategy for high performance polysulfone: ionic liquid/zwitterion as reaction medium. Green Chem. 14 (2012) 3204-3210.
6. Y. L. Liao, C. C. Hu, J. Y. Lai, Y. L. Liu, Crosslinked polybenzoxazine based membrane exhibiting in-situ self-promoted separation performance for pervaporation dehydration on isopropanol aqueous solutions. J. Memb. Sci. 531 (2017) 10-15.
7. A. Wolińska-Grabczyk, P. Kubica, A. Jankowski, M. Wójtowicz, J. Kansy, M. Wojtyniak, Gas and water vapor transport properties of mixed matrix membranes containing 13X zeolite. J. Memb. Sci. 526 (2017) 334-347.
8. Y. Ying, D. Liu, W. Zhang, J. Ma, H. Huang, Q. Yang, C. Zhong, High-Flux Graphene Oxide F. Cacho-Bailo, I. Matito-Martos, J. Perez-Carbajo, M. Etxeberría-Benavides, O. Karvan, V. Sebastián, S. Calero, C. Téllez, J. Coronas, On the molecular mechanisms for the H_2/CO_2 separation performance of zeolite imidazolate framework two-layered membranes. Chem. Sci. 8 (2017) 325-333.
9. C. C. Chang, H. J. Cho, J. Yu, R. J. Gorte, J. Gulbinski, P. Dauenhauer, W. Fan, Lewis acid zeolites for tandem Diels-Alder cycloaddition and dehydration of biomass-derived dimethylfuran and ethylene to renewable p-xylene. Green Chem. 18 (2016) 1368-1376.

10. Y. Wu, Z. Xie, D. Ng, S. Shen, Z. Zhou, Poly (ether sulfone) supported hybrid poly (vinyl alcohol)-maleic acid-silicone dioxide membranes for the pervaporation separation of ethanol– water mixtures. J. Appl. Polym. Sci. 134 (2017) 44839 (1-11).
11. K. N. Han, S. Bernardi, L. Wang, D. J. Searles, Water Structure and Transport in Zeolites with Pores in One or Three Dimensions from Molecular Dynamics Simulations. J. Phys. Chem. C 121 (2017) 381-391.
12. R. Saranya, G. Arthanareeswaran, A. F. Ismail, N. L. Reddy, M. V. Shankar, J. Kweon, Efficient rejection of organic compounds using functionalized ZSM-5 incorporated PPSU mixed matrix membrane. RSC Adv. 7 (2017) 15536-15552.
13. G. Liu, Z. Jiang, K. Cao, S. Nair, X. Cheng, J. Zhao, H. Gomaa, H. Wu, F. Pan, Pervaporation performance comparison of hybrid membranes filled with two-dimensional ZIF-L nanosheets and zero-dimensional ZIF-8 nanoparticles. J. Memb. Sci. 523 (2017) 185-196.
14. A. W. Van den Berg, L. Gora, J. C. Jansen, M. Makkee, T. Maschmeyer, Zeolite A membranes synthesized on a UV-irradiated TiO_2 coated metal support: the high pervaporation performance. J. Memb. Sci. 224 (2003) 29-37.
15. K. M. Gupta, Z. Qiao, K. Zhang, J. Jiang, Seawater pervaporation through zeolitic imidazolate framework membranes: atomistic simulation study. ACS Appl. Mater. Interfaces 8 (2016) 13392-13399.
16. C. Ding, X. Zhang, C. Li, X. Hao, Y. Wang, G. Guan, ZIF-8 incorporated polyether block amide membrane for phenol permselective pervaporation with high efficiency. Sep. Purif. Technol. 166 (2016) 252-261.
17. R. Gao, Q. Zhang, R. Lv, F. Soyekwo, A. Zhu, Q. Liu, Highly efficient polymer–MOF nanocomposite membrane for pervaporation separation of water/methanol/MTBE ternary mixture. Chem. Eng. Res. Des. 117 (2017) 688-697.
18. R. Xing, F. Pan, J. Zhao, K. Cao, C. Gao, S. Yang, G. Liu, H. Wu, Z. Jiang, Enhancing the permeation selectivity of sodium alginate membrane by incorporating attapulgite nanorods for ethanol dehydration. RSC Adv. 6 (2016) 14381-14392.
19. L. Duan, N. Hu, T. Wang, H. Wang, L. Ling, Y. Sun, X. Xie, Removal of copper and lead from aqueous solution by Adsorption onto cross-linked Chitosan/Montmorillonite Nanocomposites in the presence of Hydroxyl-Aluminum Oligomeric Cations: Equilibrium, kinetic, and thermodynamic studies. Chem. Eng. Commun. 203 (2016) 28-36.
20. N. Ghobadi, T. Mohammadi, N. Kasiri, M. Kazemimoghadam, Modified poly(vinyl alcohol)/chitosan blended membranes for isopropanol dehydration via pervaporation: Synthesis optimization and modeling by response surface methodology. J. Appl. Polym. Sci. 134 (2017) 44587 (1-16).
21. I. F. J. Vankelecom, D. Depre, S. D. Beukelaer, J. B. Uytterhoeven, Influence of Zeolites in PDMS Membranes: Pervaporation of Water/Alcohol Mixtures. J. Phys. Chem. 99 (1995) 13193-13197.
22. S. Mosleh, T. Khosravi, O. Bakhtiari, T. Mohammadi, Zeolite filled polyimide membranes for dehydration of isopropanol through pervaporation process. Chem. Eng. Res. Des. 90 (2012) 433-441.
23. H. Yin, C. Y. Lau, M. Rozowski, C. Howard, Y. Xu, T. Lai, M. E. Dose, R. P. Lively, M. L. Lind, Free-standing ZIF-71/PDMS nanocomposite membranes for the recovery of ethanol and 1-butanol from water through pervaporation. J. Membr. Sci. 529 (2017) 286-292.
24. Z. Su, J. H. Chen, X. Sun, Y. Huang, X. Dong, Amine-functionalized metal organic framework (NH_2-MIL-125 (Ti)) incorporated sodium alginate mixed matrix membranes for dehydration of acetic acid by pervaporation. RSC Adv. 5 (2015) 99008-99017.
25. P. V. Naik, L. H. Wee, M. Meledina, S. Turner, Y. Li, G. Van Tendeloo, J. A. Martens, I. F. J. Vankelecom, PDMS membranes containing ZIF-coated mesoporous silica spheres for efficient ethanol recovery via pervaporation. J. Mater. Chem. A 4 (2016) 12790-12798.
26. J. Yao, H. Wang, Zeolitic imidazolate framework composite membranes and thin films: synthesis and applications. Chem. Soc. Rev. 43 (2014) 4470-4493.
27. A. A. Alomair, S. M. Al-Jubouri, S. M. Holmes, A novel approach to fabricate zeolite membranes for pervaporation processes. J. Mater. Chem. A 3 (2015) 9799-9806.

28. J. Yang, L. Li, W. Li, J. Wang, Z. Chen, D. Yin, J. Lu, Y. Zhang, H. Guo, Tuning aluminum spatial distribution in ZSM-5 membranes: a new strategy to fabricate high performance and stable zeolite membranes for dehydration of acetic acid. Chem. Commun. 50 (2014) 1465414657.
29. N. Jullok, R. Van Hooghten, P. Luis, A. Volodin, C. Van Haesendonck, J. Vermant, B. Van der Bruggen. Effect of silica nanoparticles in mixed matrix membranes for pervaporation dehydration of acetic acid aqueous solution: Plant-inspired dewatering systems. J. Clean. Prod. 112 (2016) 4879-4889.
30. M. D. Kurkuri, T. M. Aminabhavi, Pervaporation separation of water and dioxane mixtures with sodium alginate-g-polyacrylamide copolymeric membranes. J. Appl. Polym. Sci. 89 (2003) 300-305.
31. B. G. Lokesh, K. K. Rao, K. M. Reddy, K. C. Rao, P. S. Rao, Novel nanocomposite membranes of sodium alginate filled with polyaniline-coated titanium dioxide for dehydration of 1, 4-dioxane/water mixtures. Desalination 233 (2008) 166-172.
32. K. S. Krishna Rao, B. G. Lokesh, P. Srinivasa Rao, K. Chowdoji Rao, Synthesis and characterization of biopolymeric blend membranes based on sodium alginate for the pervaporation dehydration of isopropanol/water mixtures. Sep. Sci. Technol. 43 (2008) 1065-1082.
33. M. Saraswathi, K. M. Rao, M. N. Prabhakar, C. V. Prasad, K. Sudakar, H. N. Kumar, M. Prasad, K. C. Rao, M. C. Subha, Pervaporation studies of sodium alginate (SA)/dextrin blend membranes for separation of water and isopropanol mixture. Desalination 269 (2011) 177183.
34. S. T. Udaya, T. M. Aminabhavi, Pervaporation separation of water-isopropyl alcohol mixtures with blend membranes of sodium alginate and poly (acrylamide)-grafted guar gum. J Appl Polym. Sci. 85 (2002) 2014-2024.
35. M. Y. Kariduraganavar, A.A. Kittur, S.S. Kittur, S.S. Kulkarni, K. Ramesh, Development of novel pervaporation membranes for the separation of water-isopropanol mixtures using sodium alginate and NaY zeolite. J. Membr. Sci. 238 (2004) 165-175.
36. S. D. Bhat, B.V.K. Naidu, G.V. Shanbhag, S.B. Halligudi, M. Sairam, T.M. Aminabhavi, Mesoporous molecular sieve (MCM-41)-filled sodium alginate hybrid nanocomposite membranes for pervaporation separation of water–isopropanol mixtures. Sep. Pur. Tech. 49 (2006) 56-63.
37. G. B. Thorat, S. Gupta and Z. V. Murthy, Synthesis, characterization and application of PVA/ionic liquid mixed matrix membranes for pervaporation dehydration of isopropanol. Chin. J. Chem. Eng. (2017) doi:10.1016/j.cjche.2017.02.011.
38. Z. L. Xiu, A. P. Zeng, Present state and perspective of downstream processing of biologically produced 1, 3-propanediol and 2, 3-butanediol. Appl. Microbiol. Biotechnol. 78 (2008 917926.
39. W. Zhang, Y. Ying, J. Ma, X. Guo, H. Huang, D. Liu, C. Zhong, Mixed matrix membranes incorporated with polydopamine-coated metal-organic framework for dehydration of ethylene glycol by pervaporation. J. Membr. Sci. 527 (2017) 8-17.
40. H. Wu, T. Zhou, X. Li, C. Zhao, Z. Jiang, Enhancing the separation performance by introducing bioadhesive bonding layer in composite pervaporation membranes for ethanol dehydration. Chin. J. Chem. Eng. 23 (2015) 372-378.
41. H. R. Mehta, Z. V. P. Murthy, Preparation of Sodium Montmorillonite Clay Loaded Poly(Vinyl Alcohol)-Chitosan Composite Mixed Matrix Membranes and Their Application in Pervaporation Dehydration of Isopropanol. J. Polym. Mater. 33 (2016) 319-331.

